ROCK1 mediates leukocyte recruitment and neointima formation following vascular injury

Kensuke Noma,[1] Yoshiyuki Rikitake,[1] Naotsugu Oyama,[1] Guijun Yan,[2] Pilar Alcaide,[3] Ping-Yen Liu,[1] Hongwei Wang,[1] Daniela Ahl,[1] Naoki Sawada,[1] Ryuji Okamoto,[1] Yukio Hiroi,[1] Koichi Shimizu,[4] Francis W. Luscinskas,[3] Jianxin Sun,[2] and James K. Liao[1]

[1]Vascular Medicine Research Unit, Department of Medicine, Brigham and Women's Hospital and Harvard Medical School, Boston, Massachusetts, USA. [2]Department of Cell Biology and Molecular Medicine, University of Medicine and Dentistry of New Jersey, New Jersey Medical School, Newark, New Jersey, USA. [3]Center for Excellence in Vascular Biology, Department of Pathology, Brigham and Women's Hospital and Harvard Medical School, Boston, Massachusetts, USA. [4]Donald W. Reynolds Cardiovascular Clinical Research Center, Department of Medicine, Brigham and Women's Hospital and Harvard Medical School, Boston, Massachusetts, USA.

Although Rho-associated kinase (ROCK) activity has been implicated in cardiovascular diseases, the tissue- and isoform-specific roles of ROCKs in the vascular response to injury are not known. To address the role of ROCKs in this process, we generated haploinsufficient *Rock1* (*Rock1*$^{+/-}$) and *Rock2* (*Rock2*$^{+/-}$) mice and performed carotid artery ligations. Following this intervention, we found reduced neointima formation in *Rock1*$^{+/-}$ mice compared with that of WT or *Rock2*$^{+/-}$ mice. This correlated with decreased vascular smooth muscle cell proliferation and survival, decreased levels proinflammatory adhesion molecule expression, and reduced leukocyte infiltration. In addition, thioglycollate-induced peritoneal leukocyte recruitment and accumulation were substantially reduced in *Rock1*$^{+/-}$ mice compared with those of WT and *Rock2*$^{+/-}$ mice. To determine the role of leukocyte-derived ROCK1 in neointima formation, we performed reciprocal bone marrow transplantation (BMT) in WT and *Rock1*$^{+/-}$ mice. *Rock1*$^{+/-}$ to WT BMT led to reduced neointima formation and leukocyte infiltration following carotid ligation compared with those of WT to WT BMT. In contrast, WT to *Rock1*$^{+/-}$ BMT resulted in increased neointima formation. These findings indicate that ROCK1 in BM-derived cells mediates neointima formation following vascular injury and suggest that ROCK1 may represent a promising therapeutic target in vascular inflammatory diseases.

Introduction

Vascular inflammation and smooth muscle proliferation contribute to vascular remodeling and obstructive vasculopathies such as atherosclerosis and restenosis following percutaneous coronary interventions (1, 2). The inflammatory process is characterized by the activation of vascular wall cells and circulating leukocytes, leading to the recruitment and infiltration of inflammatory cells into the vessel wall (3, 4). The subsequent secretion of cytokines and growth factors from these cells leads to increased migratory, proliferative, and secretory responses of VSMCs, resulting in vascular remodeling (5). Although recent studies have shed light on some of the pathophysiological mechanisms involved in this process, the intracellular signaling pathways that link these coordinated responses in the vascular wall cells are not known.

Rho-associated kinases (ROCKs) are serine-threonine protein kinases, which contribute to many downstream effects of the Rho GTPases. Currently, there are 2 ROCK isoforms, namely ROCK1 (also referred to as ROKβ or p160ROCK) and ROCK2 (also referred to as ROKα or Rho-kinase) (6). ROCKs regulate actin cytoskeletal reorganization, focal adhesion complex formation, smooth muscle contraction, cell migration, and gene expression (7, 8). Phosphorylation of the myosin-binding subunit (MBS) of myosin light chain phosphatase (MLCP) by ROCKs leads to inhibition of MLCP activity and increase in MLC phosphorylation and smooth muscle contraction (9).

Increased ROCK activity has been implicated in several cardiovascular diseases involving abnormal smooth muscle contraction such as cerebral and coronary vasospasm (10, 11) and perhaps hypertension (9). Furthermore, because ROCKs are also involved in cellular proliferation, migration, and survival (6, 12), they may also contribute to the development of atherosclerosis and vascular inflammation (13). Indeed, inhibition of ROCKs by the ROCK inhibitors, fasudil and Y27632, has been shown to inhibit leukocyte activation and infiltration (14), decrease tumor cell metastasis and invasion (15, 16), and inhibit dissociation-induced apoptosis of human embryonic stem cells (17).

Although pharmacological inhibition of ROCKs suggest that they are important in promoting cardiovascular disease, the tissue- and isoform-specific roles of ROCKs remain to be determined. For example, previous studies with ROCK inhibitors are limited not only by their nonselectivity for ROCK isoforms, but also, when administered in vivo chronically and at higher concentrations, ROCKs cannot be distinguished from other serine-threonine protein kinases such as protein kinase A and protein kinase C (18). In addition, when given systemically, ROCK inhibitors cannot discriminate among the tissue-specific roles of ROCKs in mediating vascular disease process. Thus, a genetic approach with gene targeting of specific ROCK isoforms offers the best strategy for dissecting and understanding the isoform-specific role of ROCKs.

We have previously generated mutant mice harboring deletion of the *Rock1* allele (19). Homozygous deletion of both *Rock1* alleles leads to embryonic and postnatal lethality (20–22). However, hap-

Nonstandard abbreviations used: BMT, bone marrow transplantation; MBS, myosin-binding subunit; PCNA, proliferating cell nuclear antigen; ROCK, Rho-associated kinase.

Conflict of interest: The authors have declared that no conflict of interest exists.

Citation for this article: *J. Clin. Invest.* **118**:1632–1644 (2008). doi:10.1172/JCI29226.

Table 1
Lumenal and neointimal area of carotid arteries 4 weeks after ligation

	n	Lumen ($\times 10^3/\mu m^2$)	Intima ($\times 10^3/\mu m^2$)	Media ($\times 10^3/\mu m^2$)	IEL ($\times 10^3/\mu m^2$)	EEL ($\times 10^3/\mu m^2$)	Intima/Media ratio
Non-BMT mice							
WT sham	4	60.6 ± 10.3	0.0 ± 0.0	12.6 ± 2.8	60.6 ± 10.3	73.2 ± 8.7	0.00 ± 0.00
WT	11	16.2 ± 4.3[A,B]	26.8 ± 5.6[A,C]	26.6 ± 2.6[D]	43.0 ± 6.6	69.6 ± 9.0	0.96 ± 0.13[A,B]
Rock1$^{+/-}$ sham	4	68.0 ± 6.2	0.0 ± 0.0	12.1 ± 1.3	68.0 ± 6.2	80.1 ± 7.2	0.00 ± 0.00
Rock1$^{+/-}$	13	38.1 ± 6.1[D]	6.9 ± 3.8[D]	26.6 ± 1.8[A]	45.1 ± 5.9	71.7 ± 7.3	0.23 ± 0.11[D]
Rock2$^{+/-}$ sham	4	62.7 ± 10.9	0.0 ± 0.0	12.4 ± 1.9	62.7 ± 10.9	75.1 ± 9.5	0.00 ± 0.00
Rock2$^{+/-}$	8	20.1 ± 4.4[A,C]	31.2 ± 8.5[A,B]	31.6 ± 3.3[A]	51.2 ± 9.7	82.8 ± 12.0	0.98 ± 0.21[A,B]
BMT mice							
WT to WT sham	4	61.0 ± 9.0	0.0 ± 0.0	14.2 ± 1.5	61.4 ± 9.0	75.3 ± 7.7	0.00 ± 0.0
WT to WT	11	15.4 ± 5.7[A,C]	25.6 ± 5.3[A,B]	28.8 ± 1.5[A]	40.9 ± 6.6	69.7 ± 6.7	0.93 ± 0.19[A,B]
WT to WT *Rock1*$^{+/-}$ sham	4	64.6 ± 12.4	0.0 ± 0.0	13.6 ± 0.9	64.6 ± 12.4	78.2 ± 11.9	0.00 ± 0.00
WT to *Rock1*$^{+/-}$	9	17.6 ± 7.4[D,C]	23.1 ± 5.7[A,C]	32.0 ± 5.3[A]	40.7 ± 7.4	72.7 ± 12.3	0.76 ± 0.14[A,C]
Rock1$^{+/-}$ to WT sham	4	65.0 ± 5.3	0.0 ± 0.0	13.9 ± 2.0	65.0 ± 5.3	78.9 ± 4.2	0.00 ± 0.00
Rock1$^{+/-}$ to WT	14	39.1 ± 6.4[D]	8.6 ± 1.9[A]	30.3 ± 3.4[A]	47.6 ± 7.8	77.9 ± 10.6	0.27 ± 0.05

The ratio of intima to media was calculated as the intimal area/medial area. All results are presented as mean ± SEM. EEL, external elastic lamina; IEL, internal EL. [A]$P < 0.01$ versus sham control in each group. [B]$P < 0.01$ versus *Rock1*$^{+/-}$ ligated vessel in non-BMT or *Rock1*$^{+/-}$ to WT ligated vessel in BMT mice. [C]$P < 0.05$ versus *Rock1*$^{+/-}$ ligated vessel in non-BMT or *Rock1*$^{+/-}$ to WT ligated vessel in BMT mice. [D]$P < 0.05$ versus sham control in each group.

loinsufficient ROCK1-knockout (*Rock1*$^{+/-}$) mice are fertile and phenotypically normal with half of the protein level of ROCK1 (20). In addition, we have generated mice with heterozygous deletion of *Rock2* allele (*Rock2*$^{+/-}$). Although the homozygous ROCK2-knockout (*Rock2*$^{-/-}$) mice die embryonically due to placental dysfunction and intrauterine growth retardation, *Rock2*$^{+/-}$ mice similarly develop normally, despite having half of the protein levels of ROCK2 (23, 24). Using these haploinsufficient ROCK mutant mice and bone marrow transplantation (BMT) to isolate the effects of BM-derived inflammatory cells, we investigated the role of ROCKs in mediating neointima formation following vascular injury.

Results

Generation of Rock1$^{+/-}$ *and Rock2*$^{+/-}$ *mice*. ROCK1-knockout mice on C57BL/6 background were generated and analyzed as described (19). Targeted deletion of a genomic fragment containing exon 3 of *Rock2* gene was accomplished by homologous recombination (see Supplemental Figure 1A; available online with this article; doi:10.1172/JCI29226DS1). Homozygous deletion of *Rock1* and *Rock2* results in embryonic and perinatal lethality (23, 24). However, heterozygous deletion of *Rock1* and *Rock2* leads to viable mice with approximately half of the protein levels of the corresponding ROCK isoform, with little if any compensatory changes in the other ROCK isoform (see Supplemental Figure 1D).

Decreased neointima formation and ROCK activity after carotid artery ligation in Rock1$^{+/-}$ *mice*. Basal and postligation systolic blood pressures were not different between WT, *Rock1*$^{+/-}$, and *Rock2*$^{+/-}$ mice ($n = 8$ in each group; P = NS). Following ligation of the common carotid artery, the vessel typically undergoes inflammatory changes, shrinkage, neointima formation, and narrowing of the lumen (25). No neointima formation and lumenal narrowing were observed in the unligated right common carotid arteries of WT, *Rock1*$^{+/-}$, and *Rock2*$^{+/-}$ mice (sham controls) (Table 1 and Figure 1A). In contrast, flow cessation caused by ligation of the left common carotid artery led to substantial increase in neointima formation in WT and *Rock2*$^{+/-}$ mice, but to a smaller increase in *Rock1*$^{+/-}$ mice ($P < 0.05$ compared with WT and *Rock2*$^{+/-}$ mice). Most of the cells in the neointima are VSMCs (data not shown, smMHC staining). This was associated with decrease in intima to media ratio in *Rock1*$^{+/-}$ mice (0.23 ± 0.11) compared with that of WT (0.96 ± 0.13) or *Rock2*$^{+/-}$ mice (0.98 ± 0.21) and a reciprocal increase in lumen size in vessels of *Rock1*$^{+/-}$ mice ($P < 0.05$ compared with WT and *Rock2*$^{+/-}$ mice) (Table 1). The medial areas as well as the areas surrounded by the external elastic lamina (EEL) and internal EL (IEL) were similar in WT, *Rock1*$^{+/-}$, and *Rock2*$^{+/-}$ vessels (P = NS). These findings suggest that ROCK1, but not ROCK2, contributes to neointima formation following vascular injury. Based upon these findings, further investigations were focused on determining the mechanisms underlying the tissue-specific role of ROCK1 in neointima formation.

Using a specific phospho-MBS antibody that corresponds to ROCK activity (19, 20), we found increased staining of the medial and neointimal areas as well as adventitia following carotid ligation of WT but not *Rock1*$^{+/-}$ mice (Figure 1B). This correlated with decreased ROCK1 expression in the vascular wall of *Rock1*$^{+/-}$ mice compared with that of WT mice. The level of staining for total MBS in the media was similar between WT and *Rock1*$^{+/-}$, mice indicating that decreased ROCK activity in *Rock1*$^{+/-}$ mice was not due to decreased substrate availability. Indeed, by western blotting, overall ROCK activity was decreased in ligated carotid arteries from *Rock1*$^{+/-}$ mice compared with that of WT or *Rock2*$^{+/-}$ mice (see Supplemental Figure 2, A and B). There were no compensatory changes in ROCK isoform expression in leukocytes of unligated and ligated *Rock1*$^{+/-}$ and *Rock2*$^{+/-}$ mice (Figure 2A). Similarly, there were no compensatory changes of ROCK isoform expression in unligated and ligated carotid arteries from *Rock1*$^{+/-}$ and *Rock2*$^{+/-}$ mice (Figure 2B). These findings indicate that changes in ROCK1, but not ROCK2, in leukocytes and carotid arteries correlated with reduced neointima formation.

Decreased leukocyte and macrophage recruitment to the vasculature in Rock1$^{+/-}$ *mice*. Endothelial-leukocyte interaction and leukocyte recruitment to the vascular wall contributes to the development of neointima formation and vascular inflammation (5). Ex vivo perfusion-fixed staining of the vessel wall following carotid artery

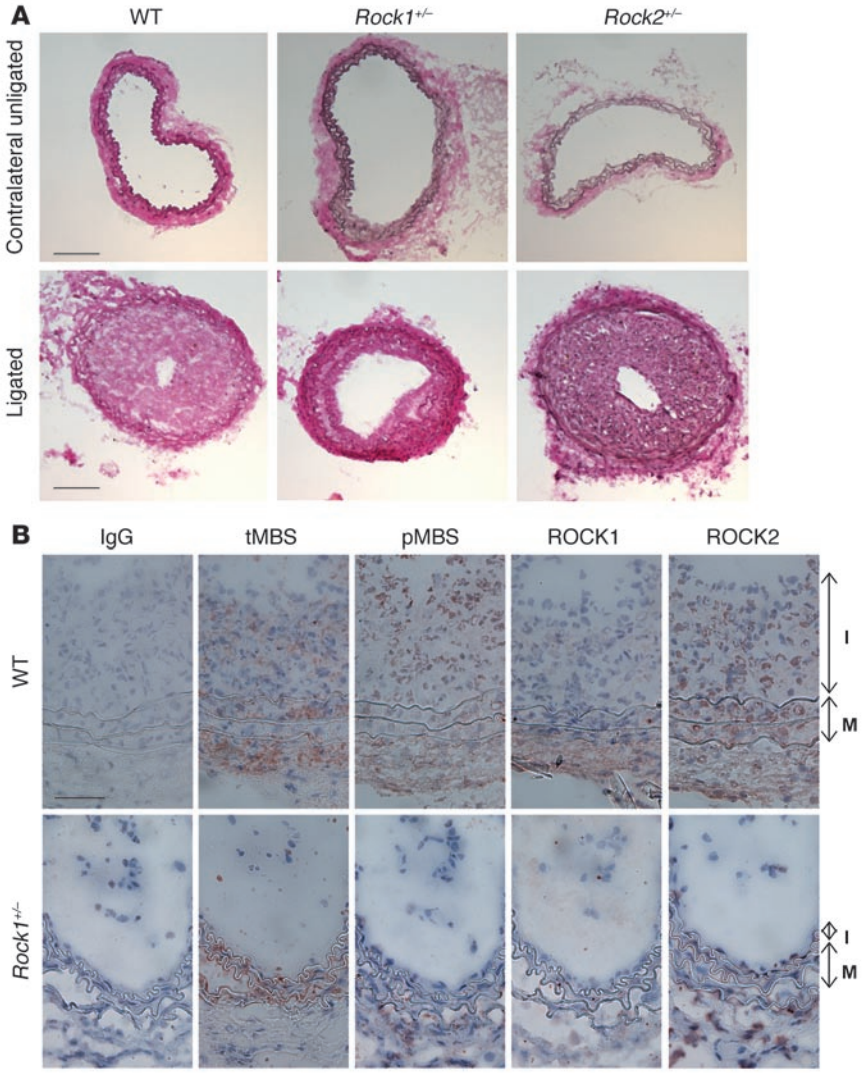

Figure 1
Decreased neointima formation after carotid artery ligation in *Rock1*$^{+/-}$ mice. (**A**) Representative cross sections of contralateral unligated and ligated carotid arteries in WT, *Rock1*$^{+/-}$, and *Rock2*$^{+/-}$ mice at 28 days after ligation. Scale bar: 100 μm. (**B**) Representative immunohistochemical analysis of ROCK expression and activity in carotid arteries from WT and *Rock1*$^{+/-}$ mice at 14 days after ligation. Vessels were stained with nonspecific antibody (IgG), and antibodies were directed at total MBS (tMBS), phosphorylated MBS (pMBS), ROCK1, and ROCK2. The I and M indicate the intima and media, respectively. Scale bar: 50 μm.

ligation was performed in a blinded manner in WT and *Rock1*$^{+/-}$ mice. Three days following carotid artery ligation, there was substantial increase in both leukocyte and macrophage accumulation in ligated arteries of WT mice compared with unligated arteries in WT and *Rock1*$^{+/-}$ mice (Figure 3). In unligated arteries, there was minimal leukocyte recruitment in either WT or *Rock1*$^{+/-}$ mice. Compared with ligated arteries of WT mice, the number of adherent leukocytes was substantially less in *Rock1*$^{+/-}$ mice compared with that of WT mice (4.3 ± 1.3 versus 14.1 ± 2.2 leukocytes/vessel section, respectively; $P < 0.05$) (Figure 3, A and B). Using MOMA-2 staining to assess macrophage accumulation, we also found less macrophage infiltration in *Rock1*$^{+/-}$ ligated vessels compared with that of WT mice (4.2 ± 0.8 versus 8.3 ± 1.2 macrophages/vessel section; $P < 0.05$) (Figure 3, C and D). These findings indicate that ROCK1 mediates leukocyte recruitment to the vessel wall after injury.

Decreased leukocyte chemotaxis, accumulation, and adherence in Rock1$^{+/-}$ *mice.* Thioglycollate-induced peritonitis in WT, *Rock1*$^{+/-}$, and *Rock2*$^{+/-}$ mice was used to assess leukocyte homing response and accumulation in vivo (26). Injection of thioglycollate increased the numbers of neutrophils and macrophages in the peritoneal cavity compared with injection of PBS (Figure 4, A and B). There was no difference in the recruitment of neutrophils and macrophages by PBS in WT, *Rock1*$^{+/-}$, and *Rock2*$^{+/-}$ mice. In contrast, neutrophil accumulation was reduced in the peritoneal cavity of *Rock1*$^{+/-}$ mice compared with that of WT and *Rock2*$^{+/-}$ mice ($7.04 \pm 0.33 \times 10^6$ versus 11.96 ± 1.02 and $10.12 \pm 1.09 \times 10^6$ neutrophils/ml, respectively; $P < 0.01$) (Figure 4A). Similarly, macrophage recruitment to the peritoneal cavity of *Rock1*$^{+/-}$ mice was also reduced compared with that of WT and *Rock2*$^{+/-}$ mice ($4.90 \pm 0.23 \times 10^6$ versus 8.35 ± 0.76 and $8.17 \pm 0.65 \times 10^6$ neutrophils/ml, respectively; $P < 0.01$) (Figure 4B). These findings suggest that neutrophil and macrophage recruitment and accumulation are impaired in *Rock1*$^{+/-}$ but not *Rock2*$^{+/-}$ mice. Indeed, compared with WT or *Rock2*$^{+/-}$ mice, VLA-4 expression is decreased by 80% in macrophages from *Rock1*$^{+/-}$ mice (see Supplemental Figure 3C).

To determine whether endothelial ROCKs could also affect monocyte adhesion, the interaction of U937 monocytes, stably expressed human L selectin (U937-LAM), with ECs from WT, *Rock1*$^{+/-}$, and *Rock2*$^{+/-}$ mice was studied under laminar flow conditions. Compared with PBS, the adherence of U937-LAM to thrombin-stimulated EC monolayers was substantially increased in ECs from WT and *Rock2*$^{+/-}$ mice ($P < 0.05$ for both).

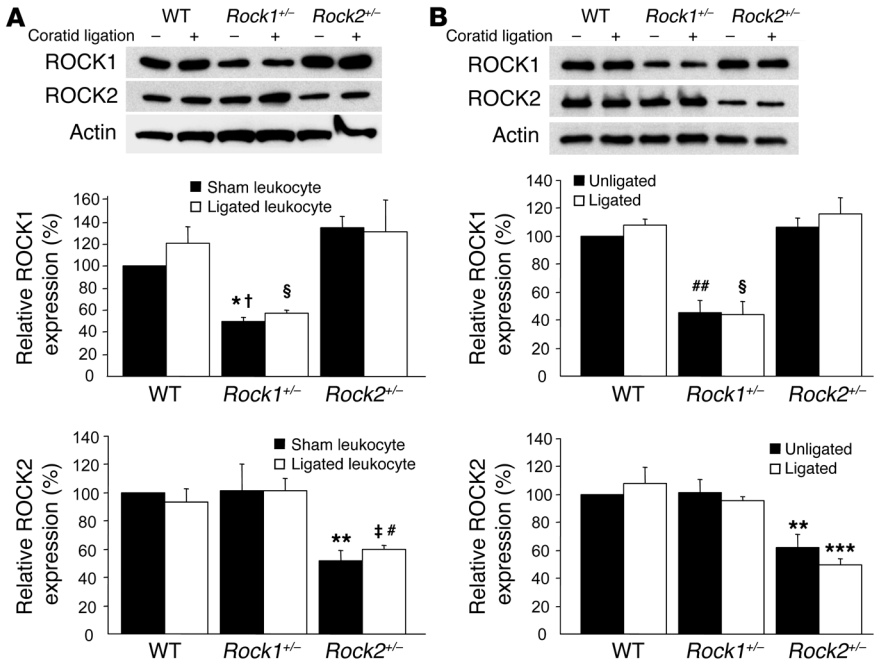

Figure 2

ROCK expression in leukocytes and carotids of *Rock1*$^{+/-}$ and *Rock2*$^{+/-}$ mice. (**A**) Expression of ROCK isoforms in leukocytes from WT, *Rock1*$^{+/-}$, and *Rock2*$^{+/-}$ mice with and without carotid ligation. Representative western blot (upper panel). Quantification of ROCK1 expression (middle panel). Mean ± SEM; $n = 3$. Quantification of ROCK2 expression (lower panel). Mean ± SEM; $n = 3$. (**B**) Expression of ROCK isoforms in unligated and ligated carotid arteries from WT, *Rock1*$^{+/-}$, and *Rock2*$^{+/-}$ mice. Representative western blot (upper panel). Quantification of ROCK1 expression (middle panel). Mean ± SEM; $n = 4$. Quantification of ROCK2 expression (lower panel). Mean ± SEM; $n = 4$. $^{*}P < 0.05$ versus unligated WT mice; $^{\dagger}P < 0.01$ versus unligated *Rock2*$^{+/-}$ mice; $^{\S}P < 0.01$ versus ligated WT and *Rock2*$^{+/-}$ mice; $^{**}P < 0.01$ versus unligated WT and *Rock1*$^{+/-}$ mice; $^{\ddagger}P < 0.01$ versus ligated WT mice; $^{\#}P < 0.05$ versus ligated *Rock1*$^{+/-}$ mice; $^{\#\#}P < 0.01$ versus unligated WT and *Rock2*$^{+/-}$ mice; $^{***}P < 0.01$ versus WT and *Rock1*$^{+/-}$ mice.

In contrast, thrombin-stimulated ECs from *Rock1*$^{+/-}$ mice do not exhibit increased U937-LAM adherence under laminar flow at either 0.5 or 1.0 dynes/cm^2 ($P < 0.01$ for both compared with WT or *Rock2*$^{+/-}$) (Figure 4, C and D). These findings suggest that endothelial ROCK1, but not ROCK2, plays an important role in mediating endothelial-leukocyte interaction in the vessel wall under physiological flow conditions.

Decreased expression of endothelial adhesion molecules in Rock1$^{+/-}$ *mice.* To determine whether ROCK1 in the vascular wall could also regulate leukocyte adhesion, the expression of adhesion molecules such as ICAM-1 and VCAM-1 was evaluated following ligation in WT and *Rock1*$^{+/-}$ mice (Figure 5, A and B). Semiqualitative analysis of immunohistochemical staining by independent blinded observers was obtained using the following scale: 0, no staining; 1, weak staining; 2, moderate staining; and 3, strong staining. Using this qualitative scale to estimate the degree of endothelial expression of adhesion molecules in WT and *Rock1*$^{+/-}$ mice compared with expression in unligated vessel, we found that ICAM-1 and VCAM-1 expression were substantially increased in ligated vessels in WT (ICAM-1, 1.3 ± 0.2; VCAM-1, 1.5 ± 0.2; $n = 10$; $P < 0.05$ for both compared with unligated vessels) but less so in *Rock1*$^{+/-}$ mice (ICAM-1, 0.5 ± 0.2; VCAM-1, 0.7 ± 0.3; $n = 10$; $P < 0.05$ for both compared with ligated WT vessels). Little or no expression of ICAM-1 or VCAM-1 was observed in the unligated vessels ($n = 5$ in each group). These findings indicate that ROCK1 mediates ICAM-1 and VCAM-1 expression in the vessel wall following vascular injury.

To confirm that ROCK1 mediates endothelial expression of ICAM-1 and VCAM-1, we isolated primary ECs from WT and *Rock1*$^{+/-}$ mice and tested their response to thrombin. In ECs from WT mice, thrombin induced the mRNA expression of *Icam1* and *Vcam1* (Figure 5C). In contrast, thrombin had little or no effect on inducing the mRNA expression of *Icam1* or *Vcam1* in ECs from *Rock1*$^{+/-}$ mice. Western blot analysis showed that the protein levels of ROCK1 in ECs from *Rock1*$^{+/-}$ mice were approximately half of that of ECs from WT mice (54.6% versus WT; $P < 0.01$) ($n = 4$), and ROCK1 expression was not affected by thrombin stimulation (Figure 5D). ROCK2 protein levels in ECs from WT and *Rock1*$^{+/-}$ mice were comparable, again suggesting no compensatory changes in endothelial ROCK2 expression in *Rock1*$^{+/-}$ mice. Thrombin increased ROCK activity within 5 minutes in ECs from WT mice (Figure 5E). However, the effect of thrombin on ROCK activity was substantially reduced in ECs from *Rock1*$^{+/-}$ mice. In contrast, thrombin-induced extracellular signal-regulated kinase (ERK) phosphorylation was relatively similar, if not somewhat higher in ECs from *Rock1*$^{+/-}$ mice compared with ECs of WT mice (Figure 5E). These findings suggest that the observed decrease in the recruitment of leukocytes to the vascular wall following carotid artery ligation in *Rock1*$^{+/-}$ mice may in part be due to the reduction in endothelial adhesion molecule expression in *Rock1*$^{+/-}$ mice.

Decreased macrophage NF-κB activation and PDGF expression in Rock1$^{+/-}$ *mice.* To determine the potential mechanisms underlying ROCK1-mediated neointima formation, we assessed NF-κB activation and PDGF expression in thioglycollate-induced peritoneal macrophages. Thioglycollate causes an inflammatory response and has been shown to induce NF-κB activation and PDGF expression in peritoneal macrophages (27, 28). In thioglycollate-induced *Rock1*$^{+/-}$ macrophages, higher steady-state level of IκB-α was observed compared with that of WT and *Rock2*$^{+/-}$ macrophages (Figure 6A). This corresponded to decreased NF-κB activation in thioglycollate-induced *Rock1*$^{+/-}$ macrophages (Figure 6B). Similarly, *Pdgfa* but not *Pdgfa* expression in thioglycollate-induced macrophages from *Rock1*$^{+/-}$ mice was reduced compared with those from WT and *Rock2*$^{+/-}$ mice ($P < 0.05$) (Figure 6C). These findings suggest that the regulation of NF-κB activation and PDGF-A expression by ROCK1 in macrophages may mediate some of the vascular inflammatory response to injury.

Decreased VSMC proliferation in the neointima of Rock1$^{+/-}$ *mice.* To determine the local vascular effects of ROCK1 on neointima formation, we assessed the degree of cellular proliferation in the vas-

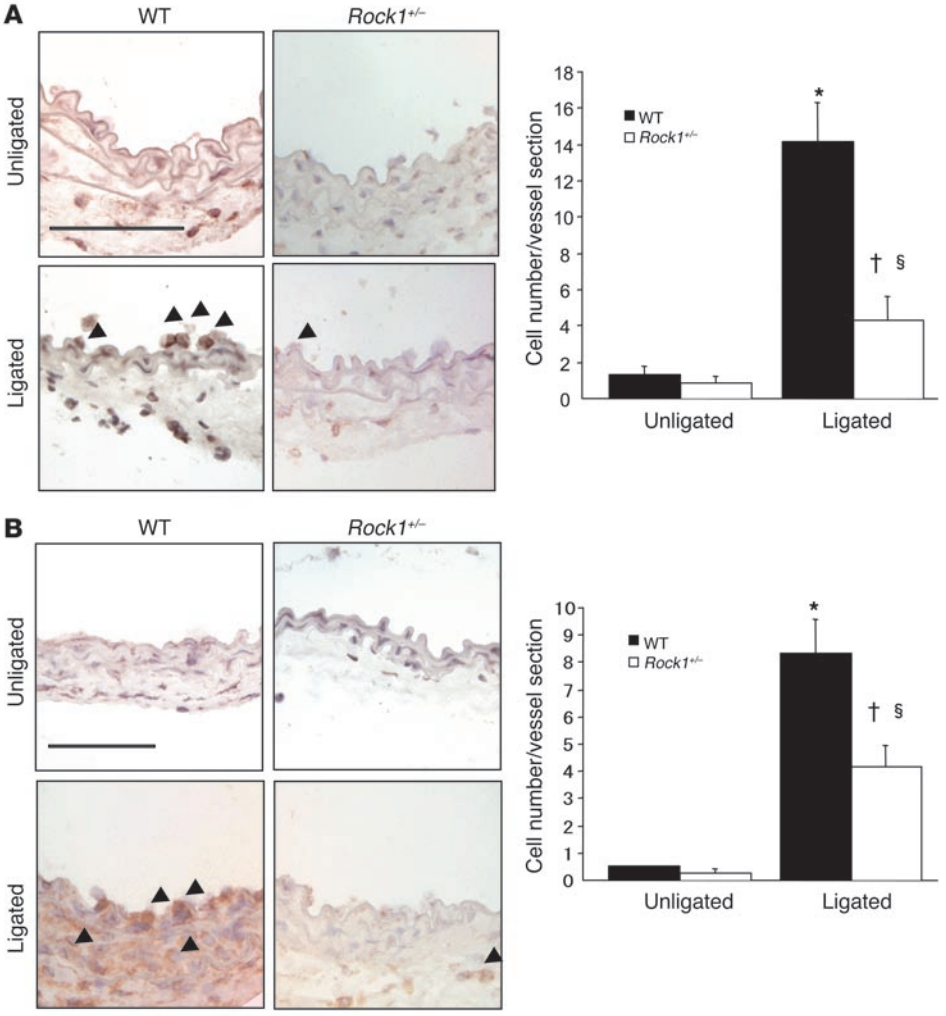

Figure 3
Decreased leukocyte recruitment to ligated vessels of *Rock1*$^{+/-}$ mice. (**A**) Representative histological sections from carotid arteries in WT and *Rock1*$^{+/-}$ mice stained with CD45 Ab for leukocytes. Arrowheads indicate CD45-positive cells. Scale bar: 50 μm (left panel). Quantitative analysis of the number of CD45-positive leukocytes adherent to the unligated (n = 3–4 in each group) and ligated vessel walls (n = 14 in each group) at 3 days after ligation (right panel). (**B**) Representative histological sections from carotid arteries in WT and *Rock1*$^{+/-}$ mice stained with MOMA-2 Ab for macrophage. Arrowheads indicate MOMA-2–positive cells. Scale bar: 50 μm (left panel). Quantitative analysis of the number of MOMA-2–positive macrophages infiltrated into the unligated (n = 3–4 in each group) and ligated vessel (n = 12–13 in each group) at day 3. *P < 0.01 versus unligated WT mice; †P < 0.05 versus unligated *Rock1*$^{+/-}$ mice; §P < 0.05 versus ligated WT mice.

cular wall by proliferating cell nuclear antigen (PCNA) staining. PCNA staining in the vascular wall was minimal or not observed prior to 14 days following carotid artery ligation. At day 14 after carotid ligation, the ratio of PCNA-positive cells to total cells within the arterial wall was substantially increased in WT mice compared with that of *Rock1*$^{+/-}$ mice (16.7% ± 2.7% versus 5.0% ± 3.6%; P < 0.01) (Figure 7A). Most, if not all, of the PCNA-positive cells were VSMCs (data not shown, smMHC double staining). Similarly, substantial increase in PCNA staining was observed in the media in WT mice compared with that of *Rock1*$^{+/-}$ mice (9.1% ± 2.0% versus 3.4% ± 0.9%; P < 0.01).

To determine whether the decrease in proliferation is due to the reduction in vascular inflammatory response or intrinsic decrease in the ability of SMC to proliferate in *Rock1*$^{+/-}$ mice, we isolated primary VSMCs from aortas of WT and *Rock1*$^{+/-}$ mice and tested their ability to proliferate and migrate in vitro. There was no difference in the ability of WT or *Rock1*$^{+/-}$ VSMCs to adhere to the culture dish or membranes (data not shown). Surprisingly, VSMC proliferation as determined by cell number and thymidine incorporation in response to serum or PDGF was also not different between VSMCs from WT and *Rock1*$^{+/-}$ mice (Figure 7, B and C). However, the migration of VSMCs in response to PDGF as determined using a modified Boyden chamber assay was substantially reduced in *Rock1*$^{+/-}$ compared with that of WT mice (Figure 7D). Basal migration was not different between VSMCs from WT and *Rock1*$^{+/-}$ mice. These findings suggest that the increase in VSMC proliferation observed in the neointima and media following vascular injury is probably due more to the indirect increase in the vascular inflammatory response elicited by leukocytes rather than by enhanced intrinsic VSMC proliferation, since the proliferative response of VSMCs to PDGF was similar between WT and *Rock1*$^{+/-}$ mice in vitro. ROCK1, however, may contribute to increase VSMC migration and survival following vascular injury.

Similar to ECs, the expression of ROCK1 in VSMCs from *Rock1*$^{+/-}$ mice was approximately half of that in WT mice (47.7% versus WT; P < 0.01) (n = 4) (see Supplemental Figure 1E), with little or no compensatory changes in ROCK2 expression. Furthermore, thrombin stimulation did not affect ROCK1 or ROCK2 expression. In VSMCs from WT mice, PDGF increased ROCK activity as measured by phosphorylation of MBS (Figure 7E). In VSMCs from *Rock1*$^{+/-}$ mice, PDGF-induced ROCK activity was greatly reduced. PDGF-stimulated ERK phosphorylation, however, was comparable if not slightly higher in *Rock1*$^{+/-}$ mice compared with that in WT mice. These findings suggest that the decreased VSMC proliferation and neointima formation observed in *Rock1*$^{+/-}$ mice are probably not mediated by ERK.

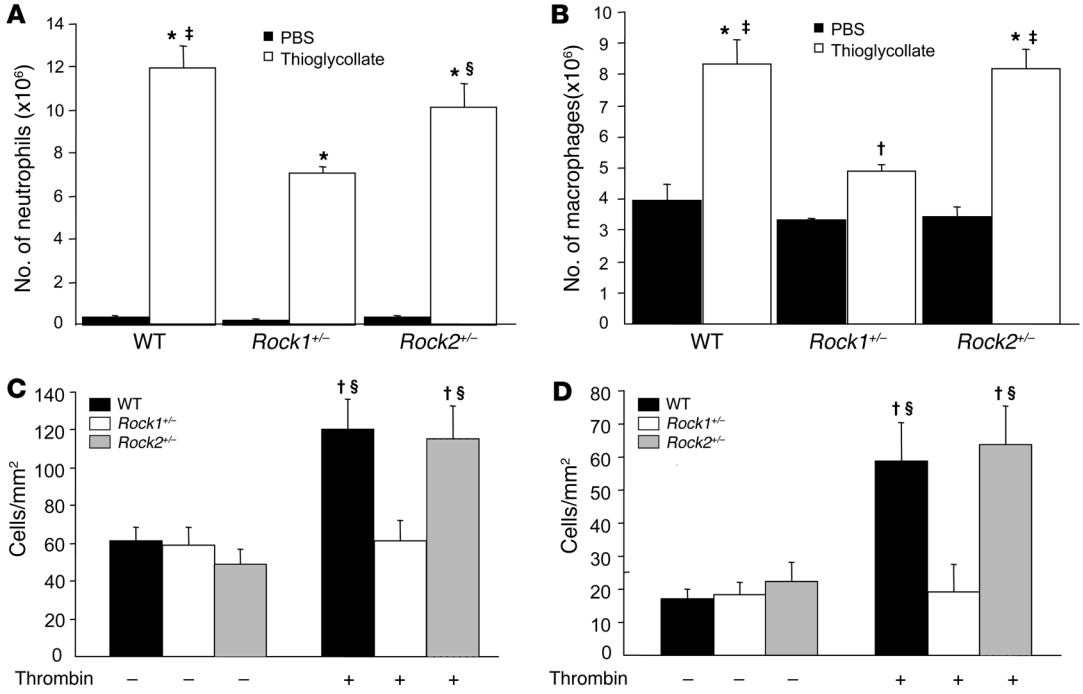

Figure 4
Decreased recruitment and adhesion of leukocytes in *Rock1*$^{+/-}$ mice. Neutrophil and macrophage recruitment was induced by i.p. injection of thioglycollate. (**A**) Neutrophil recruitment 4 hours after i.p. injection of PBS (control) or 3% thioglycollate into WT, *Rock1*$^{+/-}$, and *Rock2*$^{+/-}$ mice (n = 10, 5, and 5, respectively). (**B**) Macrophage recruitment 4 days after i.p. injection of PBS (control) or 3% thioglycollate into WT, *Rock1*$^{+/-}$, and *Rock*$^{2+/-}$ mice (n = 9, 8, and 6, respectively). Confluent monolayers of ECs isolated from WT and *Rock1*$^{+/-}$ mice were incubated with PBS (control, n = 4–6 in each group) or 10 units/ml of thrombin for 10 minutes (n = 9–10 in each group). They were then placed under laminar flow at 0.5 (**C**) or 1.0 dynes/cm^2 (**D**). U937 monocytes, stably expressed human L selectin (U937-LAM), were perfused over the EC monolayers, and adherent cells were quantified after 3 minutes. *P < 0.01 versus each control group; †P < 0.05 versus each control group; ‡P < 0.01 versus *Rock1*$^{+/-}$ mice with thioglycollate or *Rock1*$^{+/-}$ ECs with thrombin; §P < 0.05 versus *Rock1*$^{+/-}$ mice with thioglycollate or *Rock1*$^{+/-}$ ECs with thrombin.

Decreased neointima formation after carotid artery ligation by BM-derived cells from Rock1$^{+/-}$ *mice.* In contrast to arterial wire injury and transplant-associated arteriosclerosis, previous studies have shown that BM-derived cells do not contribute to neointimal VSMCs in the carotid artery ligation model (29). However, to determine the contribution of ROCK1 from BM-derived inflammatory cells to neointima formation, we performed reciprocal BMT using WT and *Rock1*$^{+/-}$ mice, using both as donors and recipients of BMT. Neither haploinsufficiency of ROCK1 nor BMT affected the total number of peripheral blood erythrocyte and leukocyte counts or leukocyte differential (see Supplemental Table 1). All mice that did not receive BMT died within 3 weeks of the transplant. Four weeks after BMT, peripheral blood counts returned to normal and the mice underwent carotid artery ligation injury. Interestingly, *Rock1*$^{+/-}$ to WT BMT mice exhibited less neointima formation and decreased intima to media ratio compared with those of WT to WT or WT to *Rock1*$^{+/-}$ BMT mice (Table 1 and Figure 8A). Indeed, neointima formation in WT to *Rock1*$^{+/-}$ BMT mice was comparable to that of WT to WT BMT mice. Circulating leukocytes isolated from WT to WT and WT to *Rock1*$^{+/-}$ BMT mice showed similar levels of ROCK1 and ROCK2 expressions compared with those of leukocytes from untransplanted WT mice, indicating successful BM replenishment (Figure 8B). Similarly, circulating leukocytes isolated from *Rock1*$^{+/-}$ to WT BMT mice showed similar levels of ROCK1 and ROCK2 expression compared with leukocytes from untransplanted *Rock1*$^{+/-}$ mice. Furthermore, ROCK2 expression in leukocytes was similar between WT to WT, WT to *Rock1*$^{+/-}$, and *Rock1*$^{+/-}$ to WT BMT mice. In contrast, ROCK1 and ROCK2 expression in ECs from WT to WT or *Rock1*$^{+/-}$ to WT BMT mice was similar to that from WT mice (Figure 8C), indicating that BMT did not affect the expression of ROCK1 and ROCK2 in the vascular wall. These findings indicate that ROCK1 in circulating leukocytes rather than in vascular wall cells is the predominant mediator of neointima formation following carotid ligation.

Decreased leukocyte recruitment to the vessel wall in Rock1$^{+/-}$ *BMT mice.* The role of leukocyte ROCK1 in mediating leukocyte recruitment to the vascular wall was evaluated 3 days following carotid artery ligation in BMT mice. The number of adherent leukocytes to the vascular wall in *Rock1*$^{+/-}$ to WT BMT mice (4.8 ± 1.1 leukocytes/vessel section) was substantially less compared with that of WT to WT (11.1 ± 1.3 leukocytes/vessel section; P < 0.01) and WT to *Rock1*$^{+/-}$ BMT mice (9.6 ± 1.8 leukocytes/vessel section; P < 0.05) (Figure 9A). In addition, there was less macrophage infiltration in vascular wall of *Rock1*$^{+/-}$ to WT BMT mice (3.4 ± 0.5 leukocytes/vessel section) compared with that of WT to *Rock1*$^{+/-}$ BMT mice (7.8 ± 1.8 leukocytes/vessel section) and WT to WT BMT mice (8.9 ± 2.4 leukocytes/vessel section) (P < 0.05) (Figure 9B). However, the expression of ICAM-1 and VCAM-1 in the vascular wall was similar between WT to WT BMT mice (ICAM-1, 1.3 ± 0.2; VCAM-1, 1.6 ± 0.2; n = 9) and *Rock1*$^{+/-}$ to WT BMT mice (ICAM-1, 0.9 ± 0.2;

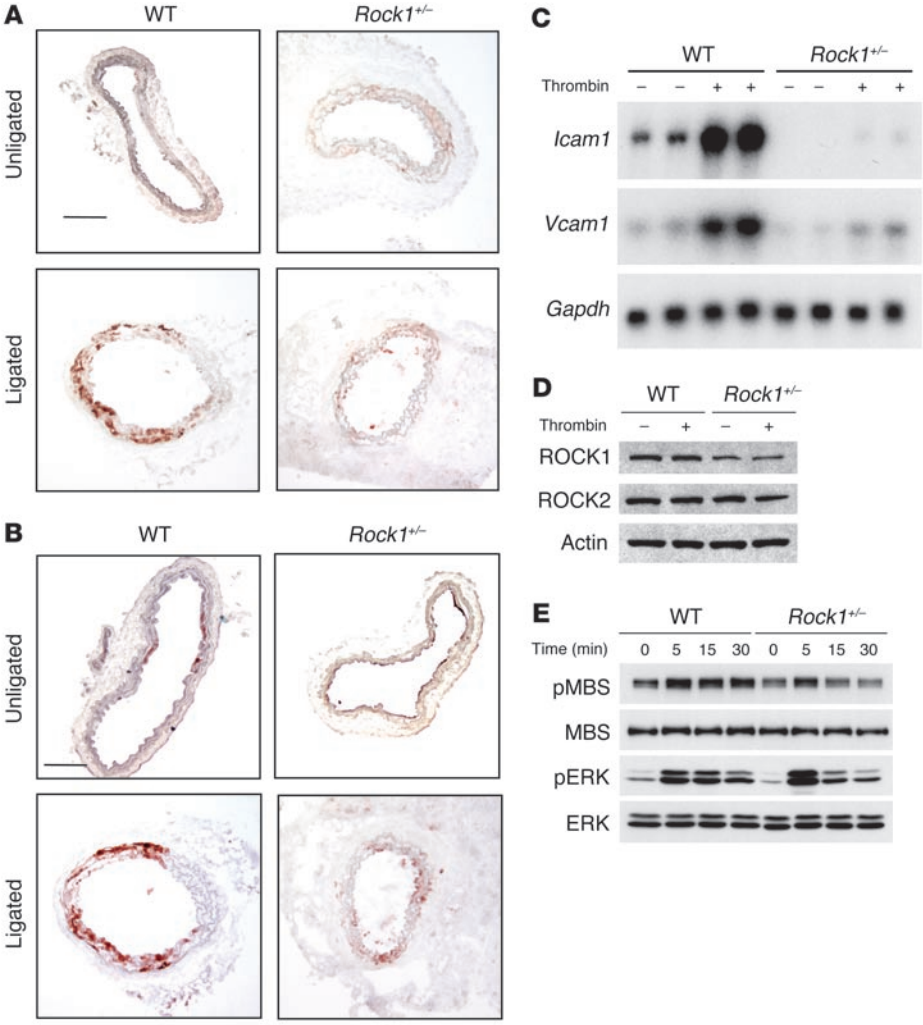

Figure 5
Decreased expression of endothelial adhesion molecules in *Rock1*$^{+/-}$ mice. Representative histological sections from unligated and ligated carotid arteries at 7 days after ligation in WT and *Rock1*$^{+/-}$ mice stained for ICAM-1 (**A**) and VCAM-1 (**B**). Scale bars: 50 μm. (**C**) Representative result of northern blot analysis of *Icam1* and *Vcam1* mRNA expression in ECs from WT and *Rock1*$^{+/-}$ mice. ECs were stimulated with 5 U/ml of thrombin for 6 hours. *Gapdh* mRNA expression was used as an internal control. (**D**) Representative result of western blot analysis of ROCK1 and ROCK2 expressions in ECs from WT and *Rock1*$^{+/-}$ mice with or without thrombin stimulation for 5 minutes. Actin was used as an internal control. (**E**) Representative result of western blot analysis of ROCK and ERK activities in ECs from WT and *Rock1*$^{+/-}$ mice. ECs were stimulated with 5 U/ml of thrombin for the indicated time periods.

VCAM-1, 1.2 ± 0.2; $n = 10$) (P = NS) (see Supplemental Figure 3, A and B). Adhesion molecule expression in the vascular wall, however, was decreased in WT to *Rock1*$^{+/-}$ mice (ICAM-1, 0.6 ± 0.2; VCAM-1, 0.8 ± 0.2; $n = 11$; $P < 0.05$ compared with WT to WT and WT to *Rock1*$^{+/-}$ BMT mice).

Following carotid artery ligation, VSMC proliferation was evaluated in the vascular wall of these BMT mice. At day 14, the ratio of PCNA-positive cells to total cells within the arterial wall was substantially reduced in the intima and media of *Rock1*$^{+/-}$ to WT BMT mice compared with those of WT to WT and WT to *Rock1*$^{+/-}$ mice ($P < 0.01$ and $P < 0.05$, respectively) (Figure 9C). These results suggest that leukocyte ROCK1 is a primary inducer of neointima formation following vascular injury since in the carotid artery ligation model, BM-derived cells do not differentiate into intimal VSMCs (29).

Discussion

Vascular remodeling is an adaptive process that occurs in response to chronic hemodynamic changes, which includes compensatory adjustment in vessel diameter and lumenal area (30). Although the precise mechanism of arterial neointima formation following vascular injury remains to be determined, growth factors, vasoactive substances, inflammatory response, adhesion molecules, and matrix modulators may all contribute to this process. Flow cessation models, such as the ligation of the common carotid artery, are useful tools for investigating the mechanism of vascular remodeling because they involve leukocyte infiltration, neointima formation, and luminal narrowing. Using this model, we have shown that vascular inflammation and neointima formation after flow cessation–induced vascular injury are substantially reduced in *Rock1*$^{+/-}$ mice compared with those of WT or *Rock2*$^{+/-}$ mice. These findings suggest a critical role for ROCK1 in the development of the neointima. It should be noted that these effects were unrelated to changes in blood pressure since systolic blood pressures were comparable among WT, *Rock1*$^{+/-}$, and *Rock2*$^{+/-}$ mice. Thus, targeting ROCK1, rather than ROCK2, may be therapeutically beneficial in reducing neointima formation following vascular injury.

Several mechanisms contribute to the observed changes in *Rock1*$^{+/-}$ ligated vessels, including inhibition of endothelial adhesion molecule expression, impaired migratory response and survival of VSMCs, and decreased leukocyte recruitment and accumulation in the vessel wall. Although ROCK2 expression was similar in ECs and VSMCs of WT and *Rock1*$^{+/-}$ mice, total ROCK activity, as defined by the phosphorylation of MBS in the vessel wall, was reduced in ligated vessels from *Rock1*$^{+/-}$ mice compared with that of WT mice. Thus, the decrease in vascular ROCK activity observed in

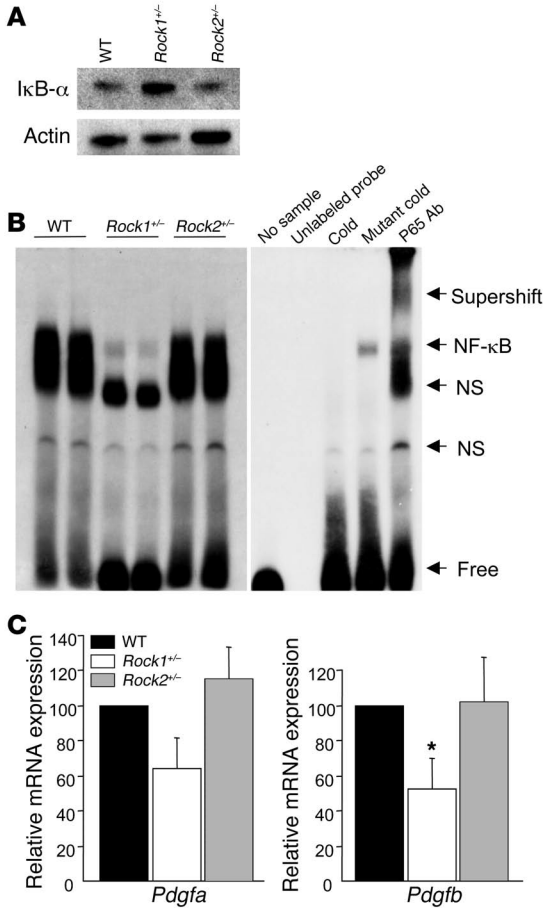

Figure 6
Decreased expression of PDGF-B, degradation of IκB-α, and activation of NF-κB in macrophages from *Rock1*$^{+/-}$ mice. (**A**) Representative western blot analysis of IκB-α expression in peritoneal macrophages from WT, *Rock1*$^{+/-}$, and *Rock2*$^{+/-}$ mice. Actin was used as an internal control. (**B**) Representative electrophoretic mobility shift assay of NF-κB in WT, *Rock1*$^{+/-}$, and *Rock2*$^{+/-}$ macrophages (left panel). Specificity of NF-κB binding activity was analyzed by the addition of unlabeled probe, by the pretreatment with excess unlabeled probe (cold) or mutant probe (mutant cold), and by anti-p65 Ab (p65 Ab) supershift gel assay (right panel). NF-κB binding band (NF-κB), nonspecific binding band (NS), free probe (free), and the raised bands supershifted by Ab (supershift) are indicated on the right. (**C**) Expression of *Pdgfa* and *-b* were analyzed by quantitative real-time PCR. Total RNA was extracted from thioglycollate-induced peritoneal macrophages in WT, *Rock1*$^{+/-}$, and *Rock2*$^{+/-}$ mice (n = 6–8). *P < 0.05 versus WT and *Rock2*$^{+/-}$ mice.

Rock1$^{+/-}$ mice corresponded to a reduction in the vascular inflammatory response and neointima formation.

The adhesion and recruitment of leukocytes to the vessel wall are the primary contributors to the inflammatory response following vascular injury. Our finding of impaired leukocyte recruitment to the vessel wall in *Rock1*$^{+/-}$ mice is consistent with previous studies showing that ROCK inhibitors decrease leukocyte recruitment and adhesion following ischemia/reperfusion injury (31). Furthermore, ROCK inhibitors have been shown to reduce neointima formation after balloon injury in rats (32, 33). However, previous studies with ROCK inhibitors have shown that ROCK inhibitors cannot discriminate between the effects of ROCK1 and ROCK2, and at higher concentrations, cannot distinguish the effects of ROCKs from other serine-threonine protein kinases such protein kinase A or protein kinase C (18). The mechanism underlying decreased leukocyte recruitment to the vessels of *Rock1*$^{+/-}$ mice could be explained in part by decrease expression of endothelial adhesion molecules. For example, administration of blocking antibodies to ICAM-1 or VCAM-1 inhibits neointima hyperplasia after arterial injury (34, 35). Furthermore, the ROCK inhibitor, Y27632, inhibits thrombin-induced ICAM-1 expression through a NF-κB–dependent mechanism (36). However, we observed no substantial decrease in neointima formation in WT to *Rock1*$^{+/-}$ ligated vessels, in which the expression levels of ICAM-1 and VCAM-1 were substantially lower compared with those of WT to WT BMT mice. These findings suggest that the lower expression of ICAM-1 and VCAM-1 in *Rock1*$^{+/-}$ mice may be sufficient to recruit leukocytes to the vessel wall and that the decrease in leukocyte recruitment and neointima formation observed in *Rock1*$^{+/-}$ mice is primarily due to the loss of ROCK1 in leukocytes.

ROCK is also important in mediating the adhesion and transmigration of monocytes (14). Overexpression of the active form of RhoA in monocytes leads to a dramatic increase in monocyte adhesion to and migration across EC monolayers, both of which were prevented by Y27632. Similarly, Y27632 has been shown to inhibit monocyte chemoattractant protein-1–induced migration of leukocytes (37). Indeed, we found that the recruitment of leukocytes such as neutrophils and macrophages in *Rock1*$^{+/-}$ mice was substantially reduced in vivo and under physiological flow conditions. The mechanism may in part be due to decrease activation of NF-κB and VLA-4 expression in *Rock1*$^{+/-}$ macrophages. Using BMT, we were able to separate the effects of ROCK1 in BM-derived cells versus local vascular wall cells in mediating neointima formation following ligation. We found that the recruitment of donor leukocytes from *Rock1*$^{+/-}$ mice to sites of inflammation or vascular injury was impaired. This was associated with decreased neointima formation in *Rock1*$^{+/-}$ to WT BMT mice, despite comparable expression of endothelial adhesion molecules as WT to WT BMT mice. These findings suggest that ROCK1 in leukocytes may play a greater role than ROCK1 in vascular wall cells in mediating neointima formation.

Although the number of PCNA-positive cells in the intimal and medial areas were substantially reduced in *Rock1*$^{+/-}$ mice compared with that of WT mice, cellular proliferation and DNA synthesis were not different between VSMCs isolated from WT and *Rock1*$^{+/-}$ mice, although *Rock1*$^{+/-}$ VSMCs exhibited decreased migration and survival. These findings suggest that the intrinsic ability of VSMCs to proliferate in response to equal concentrations of serum or PDGF is not altered in VSMCs from *Rock1*$^{+/-}$ mice compared with that of WT mice. Indeed, the level of PDGF-induced ERK activation, which plays a critical role in cell growth, was comparable between VSMCs of WT and *Rock1*$^{+/-}$ mice. Thus, the decrease in neointimal VSMC proliferation observed in vivo in ROCK1 mice may be due more to a reduction in overall inflammatory response in the vessel wall (i.e., from decreased leukocyte recruitment) rather than the intrinsic effects of ROCK1 in VSMCs. For example, the smaller number of PCNA-positive cells observed in the vessels of *Rock1*$^{+/-}$ mice as compared with that of WT mice may be due to the decrease in leukocyte recruitment and the subsequent overall reduction in the release of inflammatory and growth stimuli in the vessel wall of *Rock1*$^{+/-}$ mice. Indeed, growth factors such as

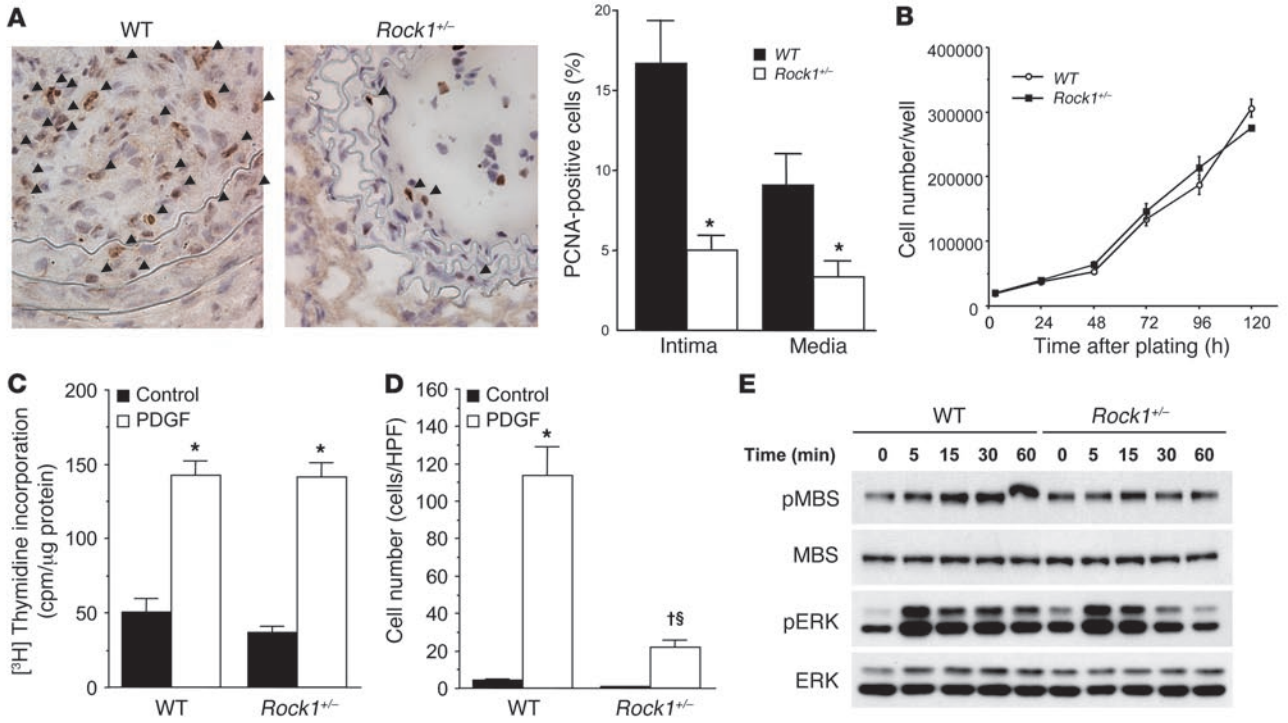

Figure 7

Decreased cell proliferation in the neointima of *Rock1*$^{+/-}$ mice. (**A**) Representative histological sections from carotid arteries in WT and *Rock1*$^{+/-}$ mice stained for PCNA at 14 days after ligation. Arrowheads indicate PCNA-positive cells. Scale bars: 50 μm (left panels). Quantitative analysis of the ratio of PCNA-positive cells to total cell number in the intima and the media (n = 10–16) (right panel). *P < 0.01 versus WT mice. (**B**) Cell proliferation in response to serum of VSMCs from WT and *Rock1*$^{+/-}$ mice. Experiments were performed 6 times in triplicates. (**C**) DNA synthesis in response to PDGF of VSMCs from WT and *Rock1*$^{+/-}$ mice (n = 12). *P < 0.01 versus without PDGF (control). (**D**) Cell migration in response to PDGF of VSMCs from WT and *Rock1*$^{+/-}$ mice (n = 8–9). *P < 0.01 versus without PDGF (control); †P < 0.01 versus control; §P < 0.01 versus WT. (**E**) Representative western blot analysis of ROCK and ERK activities in VSMCs of WT and *Rock1*$^{+/-}$ mice. VSMCs were stimulated with 10 ng/ml of PDGF for the indicated time periods.

PDGF-B are secreted from macrophages only when they are activated (38). Thus, by preventing macrophage activation, the genetic loss of ROCK1 in macrophages may lead to an overall decrease in VSMC proliferation in the vessel wall. This is consistent with our BMT studies showing that *Rock1*$^{+/-}$ to WT BMT mice have less neointima formation compared with WT to WT BMT mice. As mentioned, BM-derived cells do not differentiate into neointimal VSMCs in the carotid ligation model (29).

In summary, we have shown that ROCK1 mediates leukocyte recruitment and neointima formation following vascular injury. ROCK1 in ECs contributes to the induction of endothelial adhesion molecules, whereas ROCK1 in VSMCs mediates VSMC migration and survival. More importantly, ROCK1 in circulating leukocytes appears to be the primary determinant of leukocyte recruitment to the vessel wall and is the critical mediator of neointima proliferation. Thus, targeting ROCK1 in leukocytes may be an effective strategy for treating vascular inflammatory and proliferative diseases. Further studies are necessary to determine the precise mechanism by which ROCK1 regulates leukocyte function.

Methods

Generation of Rock1- or Rock2-knockout mice. ROCK1-knockout mice were generated on C57BL/6 background as described previously (19). Deletion of the *Rock2* allele was accomplished by homologous recombination using a targeting vector corresponding to a genomic fragment containing exon 3 of the *Rock2* gene (see Supplemental Figure 1A). Successful targeting and deletion of ROCK2 were confirmed by Southern blotting and PCR. Homozygous deletion of ROCK2 on C57BL/6 background is embryonically lethal. However, heterozygous *Rock1*$^{+/-}$ and *Rock2*$^{+/-}$ mice are viable and have half the protein levels of ROCK1 and ROCK2, respectively, without compensatory increase in the other ROCK isoform. All mice and their littermates (i.e., all on C57BL/6 background) were maintained at the Harvard Medical School animal facilities. The Standing Committee on Animals at Harvard Medical School has approved all protocols pertaining to experimentation with animals in this study.

Carotid artery ligation model. Carotid artery ligation was performed as described previously (25, 39). Male *Rock1*$^{+/-}$, *Rock2*$^{+/-}$, and littermate WT controls were used in this study. Carotid arteries were perfusion fixed through the left ventricle with 4% paraformaldehyde and 10% sucrose in PBS under physiological pressure as described previously (39).

Histology and immunostaining. Carotid arteries were embedded transversely in OCT compound (Tissue-Tek). Sections (6 μm) from animals euthanized 3, 7, 14, and 28 days after ligation were obtained at 1 mm proximal to the ligature. Elastica van Gieson staining was used for histochemical analysis to evaluate neointima formation. Two or more researchers, who were blinded to the experimental protocol, were enlisted to perform morphometric analysis using the NIH image software, ImageJ (http://rsb.info.nih.gov/ij/). Immunostaining with antiphosphospecific threonine 853 MBS (1:200)

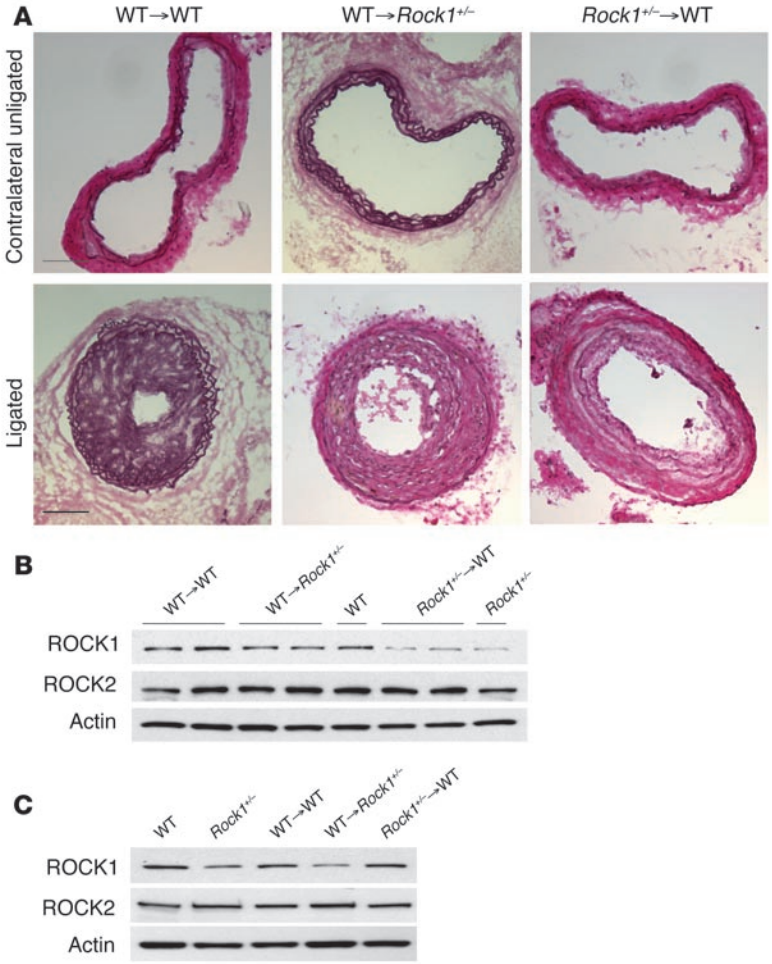

Figure 8
ROCK1 in BM-derived cells mediates to neointima formation. (**A**) Representative cross sections of contralateral unligated and ligated carotid arteries in WT to WT, WT to *Rock1*$^{+/-}$, and *Rock1*$^{+/-}$ to WT BMT mice at 28 days after ligation. Scale bars: 100 μm. Representative western blot analysis of ROCK expression in leukocytes (**B**) and ECs (**C**) from WT and *Rock1*$^{+/-}$ BMT mice. Actin was used as an internal control.

(19), anti-MBS (1:200; Covance Inc.) (19), anti-ROCK1 (1:100; Santa Cruz Biotechnology Inc.), anti-ROCK2 (1:100; Santa Cruz Biotechnology Inc.), anti–ICAM-1 (1:100; Santa Cruz Biotechnology Inc.), anti–VCAM-1 (1:100; Southern Biotechnology Associates Inc.), anti-mouse CD45 (1:100; eBioscience Inc.), and anti–MOMA-2 (1:100; Serotec Ltd.) Abs was performed. After incubation with the biotinylated Abs (Vector Laboratories), antigen-Ab complexes were visualized with horseradish peroxidase streptavidin (Vector Laboratories), followed by 9-amino-3-ethylene-carbazole (AEC; Dako Inc.) or 3,3′-diaminobenzidine (DAB; Vector laboratories). PCNA staining was performed with the use of a PCNA Staining kit (Zymed laboratories Inc.). The expression of ICAM-1 and VCAM-1 was semiquantitatively evaluated by blinded observers using the following scale: 0, negative; 1, variable or weak; 2, moderately or strongly positive.

Isolation and primary culture of mouse ECs and VSMCs. Isolation and culture of ECs and VSMCs from WT or *Rock1*$^{+/-}$ mice were described previously (19, 40). At least 2 independent preparations for each experiment were used.

Thioglycollate-induced peritonitis. Each mouse was injected i.p. with 1 ml of 3% thioglycollate (Sigma-Aldrich) as previously described (26). Four hours or 4 days after the injection, animals were killed by CO_2 asphyxiation, and 9 ml of PBS containing 0.1% of BSA, 0.5 mM EDTA, and 10 U/ml of heparin was injected i.p. Cells were recovered by peritoneal lavage. Total cell count in the lavage was determined by a Coulter counter. Cytospin (Thermo Scientific) preparations of the lavage were stained with Wright's stain and differentially counted to determine the percentage of neutrophils or macrophages. After centrifugation, harvested peritoneal cells were resuspended in DMEM plus 10% FBS and plated into appropriate wells. Cells were allowed to adhere for 2 hours and then washed free of nonadherent cells (27, 28).

Northern blotting. Northern blotting was performed as described previously (19). Primary cultures of ECs were stimulated with 5 U/ml of thrombin (Sigma-Aldrich) in 1% serum for 6 hours. Total RNA was isolated, separated on 1% agarose gel, and transferred onto nitrocellulose membrane. The oligonucleotide probes for *Icam1* and *Vcam1* were obtained as a PCR product using specific primers for murine *Icam1* (forward, 5′-CATCGGGGTGGTGAAGTCTGT-3′; reverse, 5′-TGTCGGGGGAAGTGTGGTC-3′) and *Vcam1* (forward, 5′-CAGCTAAATAATGGGGAACTG-3′; reverse, 5′-GGGCGAAAAATAGTCCTTG-3′), respectively. *Gapdh* expression was used as an internal control. Radiolabeling of probes was performed using random hexamer priming, with [α-^{32}P]CTP and Klenow fragment of DNA polymerase I (Pharmacia Corp.).

Real-time quantitative RT-PCR. Total RNA was extracted from the macrophages with TRIzol. The Quantitect SYBR Green RT-PCR kit (QIAGEN) was carried out to perform amplifications with the 1-step protocol as described by the manufacturer using an ABI Prism 7900HT sequence detector (Applied Biosystems). The following primers were used to amplify PDGF-A, PDGF-B, and GAPDH partial cDNA: *Pdgfa* (forward, 5′-TGGCTCGAAGTCAGATCCACA-3′ and reverse, 5′-AGCCCCTACGGAGTCTATCTC-3′), *Pdgfb* (forward, 5′-CGAGCCAAGACGCCTCAAG-3′ and reverse, 5′-CATGGGTGTGCTTAAACTTTCG-3′), and *Gapdh* (forward, 5′-GCAGTGGCAAAGTGGAGATT-3′ and reverse, 5′-CACATTGGGGGTAGGAACAC-3′). The fluorescence curves were analyzed with software included by Applied Biosystems. GAPDH was used as an endogenous control reference. Fold change is shown as relative to that of WT control mice.

Western blotting. Western blotting was performed using phospho-specific threonine 853 MBS polyclonal Ab (19), MBS polyclonal Ab (Covance Inc.), ROCK1 monoclonal Ab (BD Transduction Laboratories), ROCK2 monoclonal Ab (BD Transduction Laboratories), IκB-α (Santa Cruz Biotechnology Inc.), and actin polyclonal Ab (Sigma-Aldrich) as described previously (19). Primary cultures of ECs were stimulated with 5 U/ml of thrombin (Sigma-Aldrich) in 1% serum for the 5 indicated periods (see Methods and Figure 5). Also, primary cultures of VSMCs were stimulated with 10 ng/ml of human PDGF-BB in 0.4% serum-containing DMEM for the indicated periods (see Methods and Figure 7).

Electrophoretic mobility shift assay. Nuclear proteins were isolated from macrophage samples and NF-κB activity was examined by EMSA as described previously (41). A 20-μl binding reaction mixture containing 5 μg of nuclear proteins was incubated with ^{32}P-labeled double-stranded NF-κB consensus binding sequence (Santa Cruz Biotechnology Inc.) for 1 hour at 4°C. A supershift assay using antibodies to 2 μg of p65 Ab was performed to confirm NF-κB binding specificity as described previously (41).

Leukocyte adhesion under defined laminar flow conditions. Leukocyte interactions with ECs from either WT or *Rock1*$^{+/-}$ mice were examined

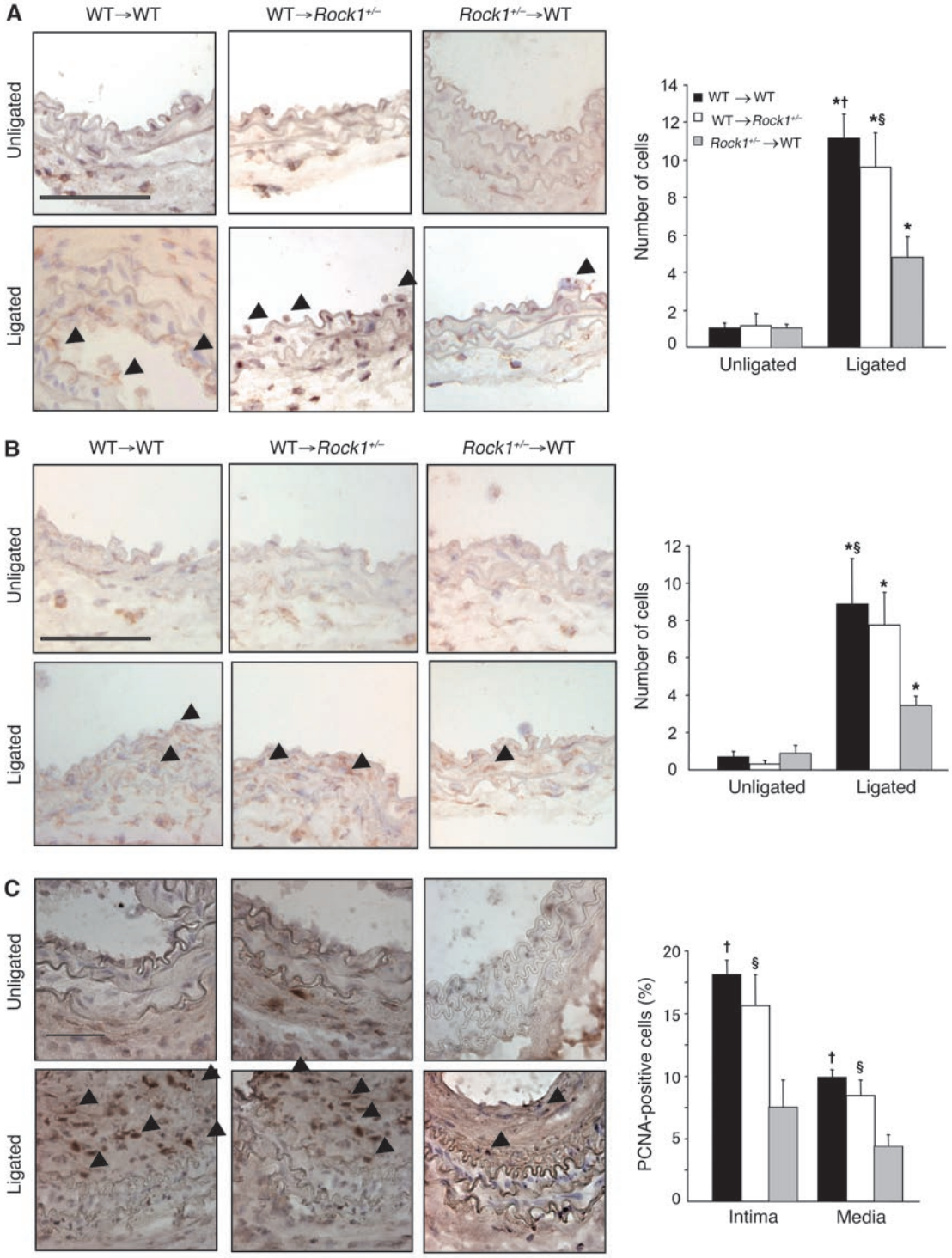

Figure 9

BM-derived cells contribute to leukocyte recruitment and cell proliferation in *Rock1*$^{+/-}$ to WT BMT mice. (**A**) Representative histological sections from carotid arteries in WT and *Rock1*$^{+/-}$ BMT mice stained with CD45 Ab for leukocytes. Arrowheads indicate CD45-positive cells. Scale bar: 50 μm (left panel). Quantitative analysis of the number of CD45-positive leukocytes adherent to the unligated (n = 3–4) and ligated vessel wall at 3 days after ligation (n = 8–12). (**B**) Representative histological sections from carotid arteries in WT and *Rock1*$^{+/-}$ BMT mice stained with MOMA-2 Ab for macrophages. Arrowheads indicate MOMA-2–positive cells. Scale bar: 50 μm (left panel). Quantitative analysis of the number of MOMA-2–positive macrophages infiltrated into the unligated (n = 3–4) and ligated vessel wall at days 3 (n = 7–8). (**C**) Representative histological sections from carotid arteries in WT and *Rock1*$^{+/-}$ BMT mice stained for PCNA at 14 days after ligation. Arrowheads indicate PCNA-positive cells. Scale bar: 50 μm (left panel). Quantitative analysis of the ratio of PCNA-positive cells to total cell number in the intima and the media (n = 8–9). $^{*}P < 0.05$ versus unligated mice; $^{\dagger}P < 0.01$, $^{\S}P < 0.05$ versus *Rock1*$^{+/-}$ to WT mice.

under conditions of fluid shear stress in a parallel plate flow chamber as described previously (41, 42).

Cell proliferation assay. Cells were plated at a density of 40,000 cells per well in 6-well dishes and cultured with or without 10 ng/ml of human PDGF-BB in 0.4% serum-containing DMEM for the indicated periods (see Methods and Figure 7). Cell numbers were quantified using an automated cell counter and each value was derived from 6 independent experiments performed in triplicate.

Thymidine incorporation. Cells were plated on to 24-well plates at a density of 20,000 cells/well and then serum-starved for 48 hours with 0.4% serum prior to stimulation for 24 hours with or without PDGF. During the last 6 hours of stimulation, cells were incubated with [^{3}H] thymidine (Amersham).

Cell migration assays. Cell migration was measured using Transwell 24-well chambers separated by a filter (8-μm pore size) coated with 0.1% gelatin. A total of 2×10^4 cells were added to the upper chamber and serum-starved for 24 hours. PDGF-BB (10 ng/ml) was added to the lower chamber and incubated for 4 hours. Cells that migrated on the filter were stained with the use of Protocol (Fisher), and cell numbers were counted using light microscopy (×200).

BMT protocol. Twenty-four male WT C57BL/6 (The Jackson Laboratory; 8 weeks old; $n = 75$) and *Rock1*$^{+/-}$ (8 weeks old; $n = 37$) mice underwent total body lethal irradiation (9.5 Gy) to eliminate endogenous BM stem cells and circulating leukocytes. BM cells used for repopulation were extracted from the femur and tibia of 10 WT and 5 *Rock1*$^{+/-}$ mice. Irradiated mice were injected intravenously with 10^7 BM cells from either WT or *Rock1*$^{+/-}$ mice. At 4 weeks after BMT, blood and leukocyte counts returned to normal (see Supplemental Table 1). Therefore, carotid artery ligation was performed 4 weeks after BMT. All irradiated mice that were not injected with transplanted BM cells die within 2–3 weeks after radiation.

Statistics. All data are expressed as the mean ± SEM. Statistical analysis was performed by unpaired 2-tailed Student's *t* test or ANOVA with a Fisher's exact post-test. A Mann-Whitney *U* test was used for comparison between groups with noncontinuous parameters, i.e., histological grading scores. A *P* value of less than 0.05 was considered statistically significant.

Acknowledgments

This work was supported by grants from the NIH (HL052233 and HL080187 to J.K. Liao; HL053993 to F.W. Luscinskas; and GM-67049, HL-67249, and HL-67283 to K. Shimizu), the American Heart Association (Bugher Foundation Award to J.K. Liao, Scientist Development Grant 0630047N to J. Sun and 0630010N to K. Shimizu, and Postdoctoral Research Fellowship to D. Ahl), the Japan Heart Foundation (Japan Heart Foundation/Bayer-Yakuhin Research Grant Abroad to K. Noma, Y. Rikitake, and N. Oyama), and the National Health Research Institute, Zhunan Town, Republic of China (to P.-Y. Liu).

Received for publication May 26, 2006, and accepted in revised form February 27, 2008.

Address correspondence to: James K. Liao, Brigham and Women's Hospital, 65 Landsdowne Street, Room 275, Cambridge, Massachusetts 02139, USA. Phone: (617) 768-8424; Fax: (617) 768-8425; E-mail: jliao@rics.bwh.harvard.edu.

Kensuke Noma, Yoshiyuki Rikitake, and Naotsugu Oyama contributed equally to this work.

1. Pasterkamp, G., Galis, Z.S., and de Kleijn, D.P. 2004. Expansive arterial remodeling: location, location, location. *Arterioscler. Thromb. Vasc. Biol.* **24**:650–657.
2. Bobik, A., and Tkachuk, V. 2003. Metalloproteinases and plasminogen activators in vessel remodeling. *Curr. Hypertens. Rep.* **5**:466–472.
3. Serrano, C.V., Jr., et al. 1997. Coronary angioplasty results in leukocyte and platelet activation with adhesion molecule expression. Evidence of inflammatory responses in coronary angioplasty. *J. Am. Coll. Cardiol.* **29**:1276–1283.
4. Tanaka, H., et al. 1993. Sustained activation of vascular cells and leukocytes in the rabbit aorta after balloon injury. *Circulation.* **88**:1788–1803.
5. Libby, P. 2002. Inflammation in atherosclerosis. *Nature.* **420**:868–874.
6. Riento, K., and Ridley, A.J. 2003. Rocks: multifunctional kinases in cell behaviour. *Nat. Rev. Mol. Cell Biol.* **4**:446–456.
7. Shimokawa, H., and Takeshita, A. 2005. Rho-kinase is an important therapeutic target in cardiovascular medicine. *Arterioscler. Thromb. Vasc. Biol.* **25**:1767–1775.
8. Noma, K., Oyama, N., and Liao, J.K. 2006. Physiological role of ROCKs in the cardiovascular system. *Am. J. Physiol. Cell Physiol.* **290**:C661–C668.
9. Uehata, M., et al. 1997. Calcium sensitization of smooth muscle mediated by a Rho-associated protein kinase in hypertension. *Nature.* **389**:990–994.
10. Sato, M., Tani, E., Fujikawa, H., and Kaibuchi, K. 2000. Involvement of Rho-kinase-mediated phosphorylation of myosin light chain in enhancement of cerebral vasospasm. *Circ. Res.* **87**:195–200.
11. Masumoto, A., et al. 2002. Suppression of coronary artery spasm by the Rho-kinase inhibitor fasudil in patients with vasospastic angina. *Circulation.* **105**:1545–1547.
12. Rikitake, Y., and Liao, J.K. 2005. ROCKs as therapeutic targets in cardiovascular diseases. *Expert Rev. Cardiovasc. Ther.* **3**:441–451.
13. Mallat, Z., et al. 2003. Rho-associated protein kinase contributes to early atherosclerotic lesion formation in mice. *Circ. Res.* **93**:884–888.
14. Honing, H., et al. 2004. RhoA activation promotes transendothelial migration of monocytes via ROCK. *J. Leukoc. Biol.* **75**:523–528.
15. Lepley, D., Paik, J.H., Hla, T., and Ferrer, F. 2005. The G protein-coupled receptor S1P2 regulates Rho/Rho kinase pathway to inhibit tumor cell migration. *Cancer Res.* **65**:3788–3795.
16. Kamai, T., et al. 2003. Significant association of Rho/ROCK pathway with invasion and metastasis of bladder cancer. *Clin. Cancer Res.* **9**:2632–2641.
17. Watanabe, K., et al. 2007. A ROCK inhibitor permits survival of dissociated human embryonic stem cells. *Nat. Biotechnol.* **25**:681–686.
18. Rikitake, Y., et al. 2005. Inhibition of Rho kinase (ROCK) leads to increased cerebral blood flow and stroke protection. *Stroke.* **36**:2251–2257.
19. Rikitake, Y., and Liao, J.K. 2005. Rho-kinase mediates hyperglycemia-induced plasminogen activator inhibitor-1 expression in vascular endothelial cells. *Circulation.* **111**:3261–3268.
20. Rikitake, Y., et al. 2005. Decreased perivascular fibrosis but not cardiac hypertrophy in ROCK1$^{+/-}$ haploinsufficient mice. *Circulation.* **112**:2959–2965.
21. Shimizu, Y., et al. 2005. ROCK-I regulates closure of the eyelids and ventral body wall by inducing assembly of actomyosin bundles. *J. Cell Biol.* **168**:941–953.
22. Zhang, Y.M., et al. 2006. Targeted deletion of ROCK1 protects the heart against pressure overload by inhibiting reactive fibrosis. *FASEB J.* **20**:916–925.
23. Thumkeo, D., et al. 2003. Targeted disruption of the mouse rho-associated kinase 2 gene results in intrauterine growth retardation and fetal death. *Mol. Cell. Biol.* **23**:5043–5055.
24. Thumkeo, D., Shimizu, Y., Sakamoto, S., Yamada, S., and Narumiya, S. 2005. ROCK-I and ROCK-II cooperatively regulate closure of eyelid and ventral body wall in mouse embryo. *Genes Cells.* **10**:825–834.
25. Mukai, Y., et al. 2006. Decreased vascular lesion formation in mice with inducible endothelial-specific expression of protein kinase Akt. *J. Clin. Invest.* **116**:334–343.
26. Mayadas, T.N., Johnson, R.C., Rayburn, H., Hynes, R.O., and Wagner, D.D. 1993. Leukocyte rolling and extravasation are severely compromised in P selectin-deficient mice. *Cell.* **74**:541–554.
27. Tavor, S., et al. 2002. Macrophage functional maturation and cytokine production are impaired in C/EBP epsilon-deficient mice. *Blood.* **99**:1794–1801.
28. Bradley, M.N., et al. 2007. Ligand activation of LXR beta reverses atherosclerosis and cellular cholesterol overload in mice lacking LXR alpha and apoE. *J. Clin. Invest.* **117**:2337–2346.
29. Tanaka, K., Sata, M., Hirata, Y., and Nagai, R. 2003. Diverse contribution of bone marrow cells to neointimal hyperplasia after mechanical vascular injuries. *Circ. Res.* **93**:783–790.
30. Geary, R.L., Kohler, T.R., Vergel, S., Kirkman, T.R., and Clowes, A.W. 1994. Time course of flow-induced smooth muscle cell proliferation and intimal thickening in endothelialized baboon vascular grafts. *Circ. Res.* **74**:14–23.
31. Wolfrum, S., et al. 2004. Inhibition of Rho-kinase leads to rapid activation of phosphatidylinositol 3-kinase/protein kinase Akt and cardiovascular protection. *Arterioscler. Thromb. Vasc. Biol.* **24**:1842–1847.
32. Sawada, N., et al. 2000. Inhibition of rho-associated kinase results in suppression of neointimal formation of balloon-injured arteries. *Circulation.* **101**:2030–2033.
33. Shibata, R., et al. 2001. Role of Rho-associated kinase in neointima formation after vascular injury. *Circulation.* **103**:284–289.
34. Oguchi, S., et al. 2000. Monoclonal antibody against vascular cell adhesion molecule-1 inhibits neointimal formation after periadventitial carotid artery injury in genetically hypercholesterolemic mice. *Arterioscler. Thromb. Vasc. Biol.* **20**:1729–1736.

35. Yasukawa, H., Imaizumi, T., Matsuoka, H., Nakashima, A., and Morimatsu, M. 1997. Inhibition of intimal hyperplasia after balloon injury by antibodies to intercellular adhesion molecule-1 and lymphocyte function-associated antigen-1. *Circulation.* **95**:1515–1522.
36. Anwar, K.N., Fazal, F., Malik, A.B., and Rahman, A. 2004. RhoA/Rho-associated kinase pathway selectively regulates thrombin-induced intercellular adhesion molecule-1 expression in endothelial cells via activation of I kappa B kinase beta and phosphorylation of RelA/p65. *J. Immunol.* **173**:6965–6972.
37. Worthylake, R.A., and Burridge, K. 2003. RhoA and ROCK promote migration by limiting membrane protrusions. *J. Biol. Chem.* **278**:13578–13584.
38. Ross, R., et al. 1990. Localization of PDGF-B protein in macrophages in all phases of atherogenesis. *Science.* **248**:1009–1012.
39. Kumar, A., and Lindner, V. 1997. Remodeling with neointima formation in the mouse carotid artery after cessation of blood flow. *Arterioscler. Thromb. Vasc. Biol.* **17**:2238–2244.
40. Sakata, Y., et al. 2004. Transcription factor CHF1/Hey2 regulates neointimal formation in vivo and vascular smooth muscle proliferation and migration in vitro. *Arterioscler. Thromb. Vasc. Biol.* **24**:2069–2074.
41. Harari, O.A., Alcaide, P., Ahl, D., Luscinskas, F.W., and Liao, J.K. 2006. Absence of TRAM restricts Toll-like receptor 4 signaling in vascular endothelial cells to the MyD88 pathway. *Circ. Res.* **98**:1134–1140.
42. Luscinskas, F.W., et al. 1994. Monocyte rolling, arrest and spreading on IL-4-activated vascular endothelium under flow is mediated via sequential action of L-selectin, beta 1-integrins, and beta 2-integrins. *J. Cell Biol.* **125**:1417–1427.